Available online at www.sciencedirect.com
ScienceDirect
Tribology International 40 (2007) 266–277
TRIBOLOGY INTERNATIONAL
www.elsevier.com/locate/triboint

Thermal stability and high-temperature wear of Ti–TiN and TiN–CrN nanomultilayer coatings under self-mated conditions

Dheepa Srinivasan[a,*], Trupti. G. Kulkarni[b], K. Anand[a]

[a]*Materials Research Laboratory, GE India Technology Center, EPIP-II, Whitefield, Bangalore 560 066, India*
[b]*National Institute of Technology Karnataka, Surathkal 575025, India*

Received 1 December 2004; accepted 1 September 2005
Available online 11 April 2006

Abstract

Ti–TiN and TiN–CrN nanomultilayers were thermally stable retaining uniform and sharp layer interfaces up to 24 h at 773 K, without any oxidation or phase transformation accompanying each individual layer. Decreasing the multilayer spacing resulted in an increase in the hardness in both cases. The coating hardness was found to be independent of the substrate type, when applied on HS718, Ti64 and HCHCr substrates. In scratch testing, the multilayers displayed a better resistance to the onset of failure, as compared to the monolayer TiN. The substrate plasticity played an important role in determining the coating failure mode. Self-mated wear tests revealed the CrN–TiN system to exhibit the best wear behaviour, both at room temperature and at 773 K. The Ti–TiN coatings are more accommodative with all three substrates, as compared to TiN–CrN and TiN.

Keywords: Nanomultilayers; Self-mated; Thermal stability

1. Introduction

A vast amount of literature has been generated in the last two decades on TiN based hard coatings and today their usefulness has been well proven in enhancing the wear resistance of cutting tools, punches and several metal-forming components. Further developments to enhance the coating performance led to the evolution of multicomponent coatings, and specifically, the multilayered coatings. Multilayers can lead to benefits in performance over comparable single-layer coatings by combining the attractive properties of different materials in a single protective layer. In recent years, multilayer coatings on the nanometer scale (nanomultilayer coatings) have proved to exhibit superior mechanical and tribological properties [1–4]. When multilayers are obtained by making the coating film as a stack of layers, and thickness of each layer vary from 1/1000 to 1/100 (between 5–20 nm) of the overall film thickness. The introduction of a number of interfaces parallel to the substrate can act to deflect cracks or provide barriers to dislocation motion, increasing the toughness and hardness of the coating. Numerous reports exist on the mechanical and tribological behaviour of these nanomultilayered coatings encompassing various nitride combinations [1–15]. However, since most of these coatings have been evaluated in view of a cutting tool application, by and large they deal with the nanomultilayers deposited on various steel or cemented carbide substrates and there is a paucity of data when it comes to other substrates, such as Ni-based or Ti-based alloys. Secondly, many of these studies deal with room temperature measurements having the coatings evaluated for their performance in the as-deposited condition. Thirdly, many a tribological test has been carried out using a softer counterface, namely steel or Al_2O_3 balls and in order to have an estimate of the limiting performance of the coating, it is best to evaluate against a harder counterface, and in the case of the TiN coatings, the ideal test would be under self-mated conditions, under a non point-loading configuration.

In order to address all three factors, the objective of the present study has been to establish the thermal

*Corresponding author. Fax: 91 80 28412111.
E-mail address: dheepa.srinivasan@geind.ge.com (D. Srinivasan).

0301-679X/$ - see front matter © 2006 Elsevier Ltd. All rights reserved.
doi:10.1016/j.triboint.2005.09.035

stability and wear behaviour of a couple of nanomultilayer combinations, at a moderate temperature of 773 K on three different substrates, in order to explore their potential in protecting other mechanical components from harsh counterfaces. This work focuses on the Ti–TiN and TiN–CrN nanomultilayer systems, and establishes the relationship between the microstructure and the wear response under self-mated conditions, at both room temperature and at 773 K.

2. Experimental details

2.1. Materials, processing and characterization (1) Ti–TiN and (2) TiN–CrN

Multilayers of 10, 20 and 100 nm individual layer spacing were deposited on to (a) tool steel (HCHCr-6 GPa hardness), (b) Ni-based (HS718-4 GPa), (c) Ti-based (Ti64-2 GPa) alloy substrates and (d) Si, using a 8 KW closed field unbalanced magnetron sputtering technique, at Teer coatings, UK. The total coating thickness was ~1–2 μm. A substrate bias of −50 V was maintained and a 100 nm Ti interlayer was deposited on all substrates prior to depositing the nanomultilayers to ensure good adhesion. All the substrates were prepared to a roughness of 0.02–0.03 μm (R_a). A TiN monolayer was also studied under identical conditions for comparison. Upon coating, the surface had the same finish as that of the substrate, 0.02–0.03 μm (R_a). In addition, comparison of the microstructure of TiN monolayer deposited via cathodic arc evaporation was made, to examine if there was any substantial difference in the coating structure between the two PVD processes. In order to map the thermal stability of the nanomultilayers, the coated samples were heat treated for various times up to 24 h, both in air and in vacuum, at 773 K. This temperature was chosen to mimic the temperature of the high-temperature tribometer test, in order to correlate the coating wear behaviour with the microstructure. The heat treatments in vacuum were performed after encapsulating the samples in a quartz tube evacuated to 10^{-6} Torr, after back filling with argon between evacuations. Annealing in air was done to correlate the microstructure with that of the tribometer test, while annealing in vacuum was done in parallel to get an understanding of the film stability in terms of interface characteristics and phase transformations, without the influence of oxidation. Preliminary phase identification of the films was done using a Philips X-ray diffractometer. Further detailed analysis of the as-deposited and annealed structures were made using a JEOL, 2010 FASTEM, 200 KV, in cross-section. The Si substrate was mainly used for ease of sample preparation in terms of time consumed for TEM cross-section samples, after ensuring that there was no difference in the structure of nanomultilayer that was deposited on Si compared to the other substrates.

3. Mechanical and tribological properties

The coating hardness was measured using a MTS nanoindentor XP, attached with a Berkovich indentor having a tip radius of 100 nm. Force modulation technique was applied to measure hardness continuously during loading, keeping the indentation depth less than 1/10th of the overall coating thickness in order to avoid substrate interference in capturing the coating hardness. Measurements were also made at depths higher than 1/10th of the coating thickness in order to compare the effect of different substrates on the combined hardness. An average of 9 indentations was taken to represent the coating hardness, with typical scatter being of the order of 3–4 GPa. Single pass scratch adhesion testing was performed using a Teer ST-200 scratch tester, having a Rockwell conical diamond indentor (tip radius of 0.2 mm), with a continuously increasing load up to 60 N, at a loading rate of $dL/dt = 100$ N/m. The critical load for coating detachment 'L_c' was determined by examining the scratch scars using the optical microscope. An average of three scratches was taken to represent the coating failure loads, with a typical scatter of ± 1 N. Unlubricated sliding wear tests were done on a CSM high-temperature tribometer, in a pin on disc configuration, with the coating present on a rotating disc (55×5 mm) rubbing against a static steel pin, 3 mm in diameter, coated with TiN monolayer, to enable a self-mated wear configuration. The TiN coating on the pin was made using the cathodic arc evaporation technique. The self-mated tests were carried out after evaluating the structures of TiN using both PVD processes and confirming that there was no significant difference. The self-mated configuration was preferred in relation to the ball on disc set up because it tends to be more representative of the loads that the coating faces in real situations during sliding wear. The tests were performed both at room temperature and at 773 K, using a normal load of 2 N, sliding speed of 0.1 m s^{-1} for a total distance of 150 m. Each test was repeated for two different radii (17 and 15 mm) and the wear rate (given by weight loss/gain) and friction coefficient was monitored. The worn surface was examined using the SEM (JEOL, 6335 FEG).

4. Results and discussion

For the sake of brevity, all the structures and stability results pertaining to only the 20 nm multilayer has been reported. The mechanical property results however, include comparisons across the different layer thicknesses.

4.1. Structure and thermal stability

Figs. 1(a)–(c) shows X-ray diffraction (XRD) patterns comparing the TiN monolayer and the multilayers, Ti–TiN and TiN–CrN, respectively. Peaks from the substrate have been identified in all cases. While the monolayer (Fig. 1(a)) exhibits a strong $(1\,1\,1)_{TiN}$ texture irrespective of the

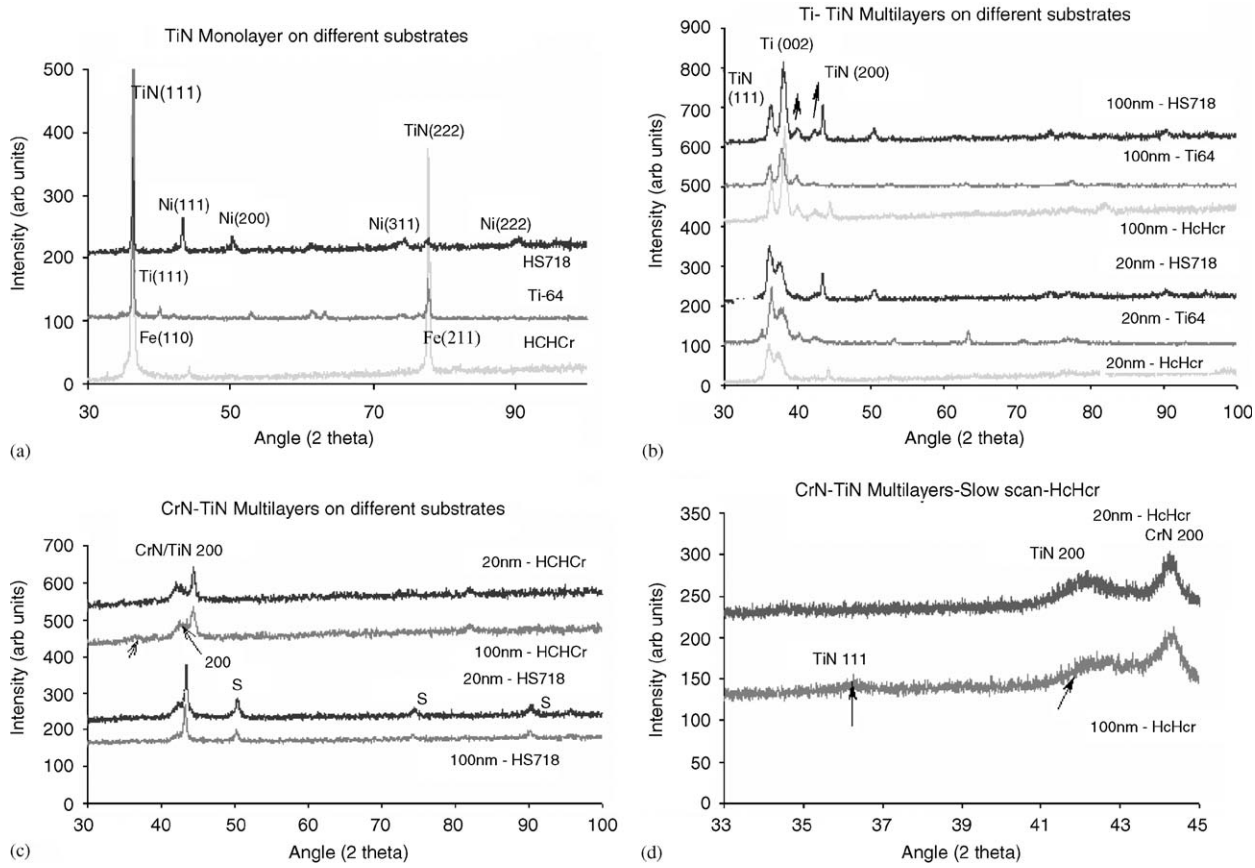

Fig. 1. XRD patterns from (a) TiN monolayer, (b)Ti–TiN, (c) TiN–CrN, multilayers (20 and 100 nm) on different substrates (HCHCr, HS718 and Ti64), and (d) slower scan revealing solid solution formation in TiN–CrN .

substrate type, it appears divided between $(1\,1\,1)_{TiN}$ and $(2\,0\,0)_{TiN}$ in the Ti–TiN multilayer. The texture appears less pronounced upon decreasing the layer thickness from 100 to 20 nm (Fig. 1(b)), where the peaks have undergone considerable broadening indicative of a grain size reduction effect. In contrast, the TiN–CrN multilayer exhibits solid-solution formation (Fig. 1(c)), whose extent gets enhanced with decreasing layer spacing, as shown in the X-ray trace in Fig. 1(d), obtained after a slow scan. Figs. 2((a)–(d)) compares the microstructure of the two types of multilayers having a 20 nm interlayer spacing, with that of the monolayer. The coating architecture comprises a 100 nm Ti interlayer between the substrate and the Ti–TiN nanomultilayer, as shown in Fig. 2(a). A columnar structure occurs in both the monolayer (Fig. 2(b)) and the multilayers (Figs. 2(c) and (d)), as evident from dark field (DF) images (insets), having a typical column width of 30–40 nm in the TiN monolayer and 100 nm in the multilayers. A gradual diminishing of the TiN texture takes place in going from the monolayer Fig. 2(b) to the Ti–TiN multilayer (Fig. 2(c)), as shown in the selected area diffraction patterns (SADP) (insets). The TiN–CrN system shows a diminishing texture (Fig. 2(d)), with the appearance of continuous polycrystalline rings, as shown in the insets. Compared to the Ti–TiN multilayers, the CrN–TiN multilayers displayed a more diffused interface. There was no significant difference between the structures of the TiN coatings deposited by the two different PVD methods, except for slightly wider columns (50–60 nm) via the cathodic arc evaporation route as compared to the magnetron sputtering (20–30 nm) (not shown). Upon annealing, all the coatings had undergone some discoloration indicative of the formation of a surface oxide, and X-ray traces had the occurrence of only peaks corresponding to TiO_2 and no Cr_2O_3 could be detected, as shown in Figs. 3(a)–(c). In addition, the heat treatment ends up in destroying the film texture to some extent, as shown in Fig. 3(a), for the TiN monolayer, which compares traces from the heat-treated coating with that of the as-deposited one. However, all the oxides and intermetallic phases seem to be occurring only on the top surface of the coating and the actual coating architecture remains unaltered, as observed from the electron micrographs (Figs. 4(a)–(d)). The columnar structure in the monolayers is intact, however, the columns have undergone some growth at this temperature to 60–70 nm (Fig. 4(a)). This is corroborated by the occurrence of single crystal diffraction patterns (inset in Fig. 4(a)), as opposed to textured rings, after the heat treatment. Both nanomultilayers seem unaffected by the heat treatment in so far as the column width and the interface sharpness is concerned (Figs. 4(b) and (c)). There definitely has been a destruction of the

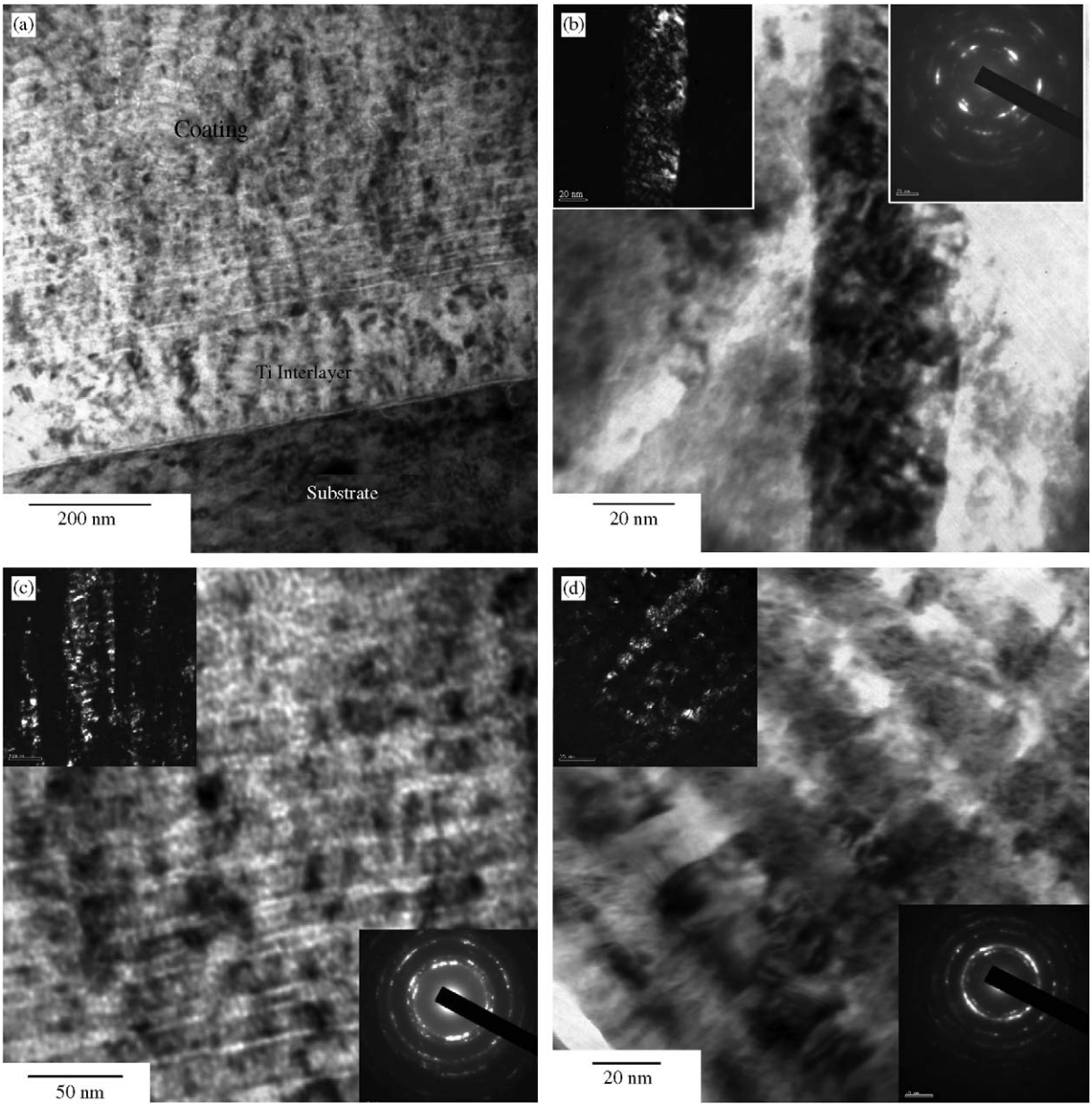

Fig. 2. As deposited microstructures showing (a) the coating architecture, (b) TiN monolayer, (c) Ti–TiN and (d) TiN–CrN multilayer, with a 20 nm interlayer spacing, on HS718 substrate. Insets show the corresponding SADP and DF image, indicating columns.

texture in the Ti–TiN coating when annealed in air (Fig. 4(c)) as compared to vacuum (Fig. 4(d)), as observed from the SADP's (insets in Fig. 4). There has been no conclusive evidence for any additional reaction product between Ti and TiN, such as Ti_2N, at each layer interface. Although there was no oxide detected between the layers, sporadic occurrence of some TiO_2 has been observed in the Ti interlayer, adjacent to the substrate, in the coating annealed in air, as shown in Fig. 4(f), whereas annealing in vacuum had no such TiO_2 formed, even in trace amounts (Fig. 4(e)). Likewise the TiN–CrN coatings (Fig. 4(b)) remain as solid solutions of alternate CrN and TiN layers, without any disruption to the individual layers up to the annealing times studied, 24 h, at 773 K. Specifically these thicknesses were chosen in order to avoid excessive intermetallic formation between interlayers, such as what has been reported for a 5 nm nanomultilayer [1].

4.2. Mechanical properties

There is no significant effect of the different substrates on the coating hardness, as shown in typical hardness curves from the Ti–TiN (20 nm) coating, Fig. 5(a). A larger indentation depth is seen to reflect the substrate type, with the final hardness being the lowest for the Ti substrate as compared to the Ni substrate followed by the steel substrate, at the highest value (Fig. 5(b)). However, the way in which the curve evolves is somewhat complicated,

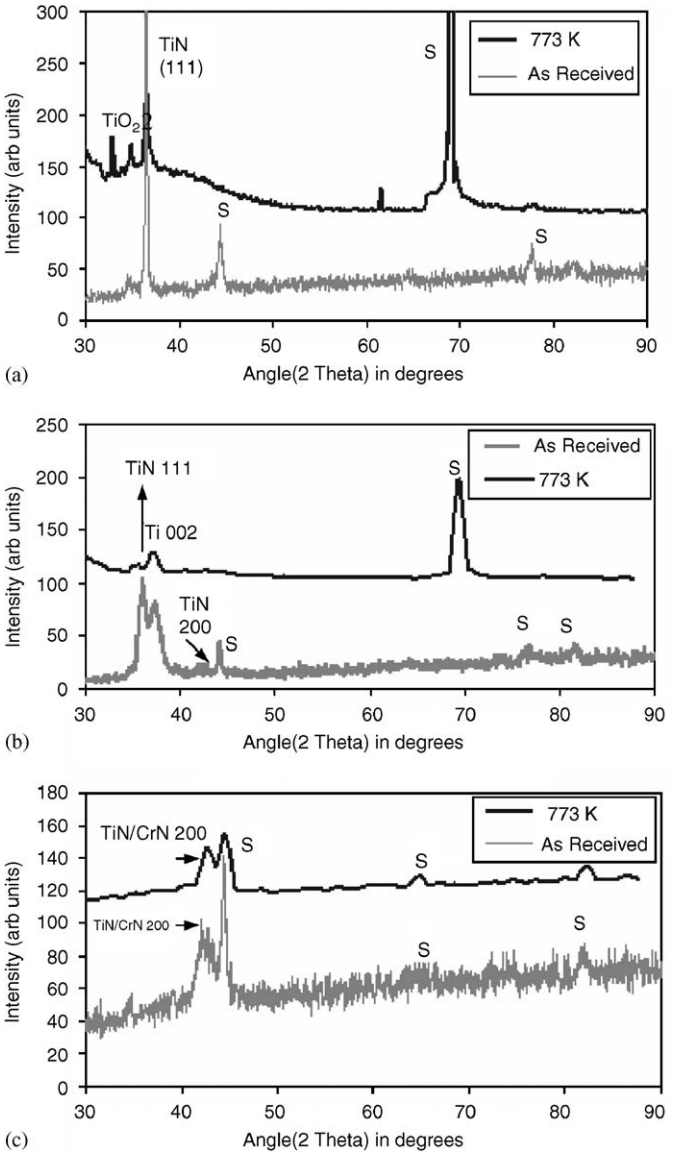

Fig. 3. X-ray traces comparing the heat treated films (on Si substrates) with the as-deposited ones (on HCHCr substrates) (a) TiN, (b) Ti–TiN and (c) TiN–CrN multilayers, with a 20 nm interlayer spacing.

through a composite effect involving both the hard coating and the softer substrate and there has been no effort in this study to decipher the same. A comparative plot of the coating hardness as a function of the layer thickness has been shown in Figs. 5(c) and (d), for the Ti–TiN and TiN–CrN coatings, respectively, on three different substrates. In both cases comparisons have been made to the monolayer TiN. The Ti–TiN multilayers show a lower hardness as compared to the monolayer TiN, however, the composite coating hardness is found to greatly exceed the value expected from a rule of mixtures. Decreasing the layer spacing results in a hardness increment in both Ti–TiN and TiN–CrN nanomultilayers, however, in the case of Ti–TiN, there seems to be a hardness peak occurring at 20 nm, amongst the three thicknesses studied, quite contrary to the popular belief that decreasing the layer spacing automatically results in a continuous increase in hardness. The hardness values of all the coatings have been listed in Table 1.

A quick way to establish the bonding between the film and the substrate is by using a single pass scratch test. Under scratch adhesion tests, the multilayers failed at much higher loads as compared to the monolayer. The latter was seen to undergo catastrophic failure with the film peeling off completely from the substrate at relatively small loads (Fig. 6(a)), whereas the failure is more gradual and well within the scratch track in both the Ti–TiN and TiN–CrN nanomultilayer coatings (Figs. 6(b) and (c)). The onset of failure in the TiN monolayer (on a HS718 substrate) along the coating-substrate edge is shown in the scanning electron micrograph in Fig. 6(d). Soon after, within a short distance, rupture of the heavily deformed TiN that initiated at defect locations, coalesced into macrocracks causing microcracking along the edge of the scratch track, ultimately leading to completely peeling of the coating as a flake, referred to as ''edge flakes'', as shown in Fig. 6(e). In contrast, in both the multilayers, the coating–substrate interface is intact and the only signs of coating failure are spotted within the scratch track, having fine microcracks initiated, leading to chipping of the track in some portions leaving those portions uncovered, as shown in Fig. 6(f). This difference in coating failure between the multilayers and the monolayer is not peculiar to the HS718 substrate alone and holds good for the other two substrates as well. However, there does exist a difference between the monolayer and the multilayers in the mode of failure on the three different substrates. While the TiN coating on the two harder substrates (HCHCr) exhibits edge flaking (Figs. 7(a) and (b)), total failure takes place by spallation or buckling ahead of the indentor in the softer substrate (Ti64), as shown in the scratch track in Fig. 7(c). At no instance, there has been adhesive failure of the monolayer on any of the three substrates. Loads corresponding to the onset of failure and complete coating failure for all three coating types have been listed in Table 1.

The multilayers are not only able to withstand the force of the diamond stylus up to much higher loads, but also exhibit far greater adherence to all three substrates. In the case of Ti–TiN there is no difference in the loads to failure or failure modes with respect to the different substrates, as shown in Figs. 7((d)–(f)). It is clear that the coating has been dragged forward by the stylus (Fig. 7(f)) leading to the conclusion that an adhesive failure had occurred. Another evidence to support this type of failure comes from the cracks observed in the track along the trailing edge. These cracks occur in a direction counterintuitive to that of the diamond indentor direction (Fig. 7(e)) brought about by the traction in the track set ahead of the indentor. The 20 nm interlayer coating performed the best, in terms of sustaining the highest critical loads to failure, on all three substrates, as shown in the comparative failure plots in Figs. 8((a) and (b)). In both Ti–TiN and TiN–CrN, there

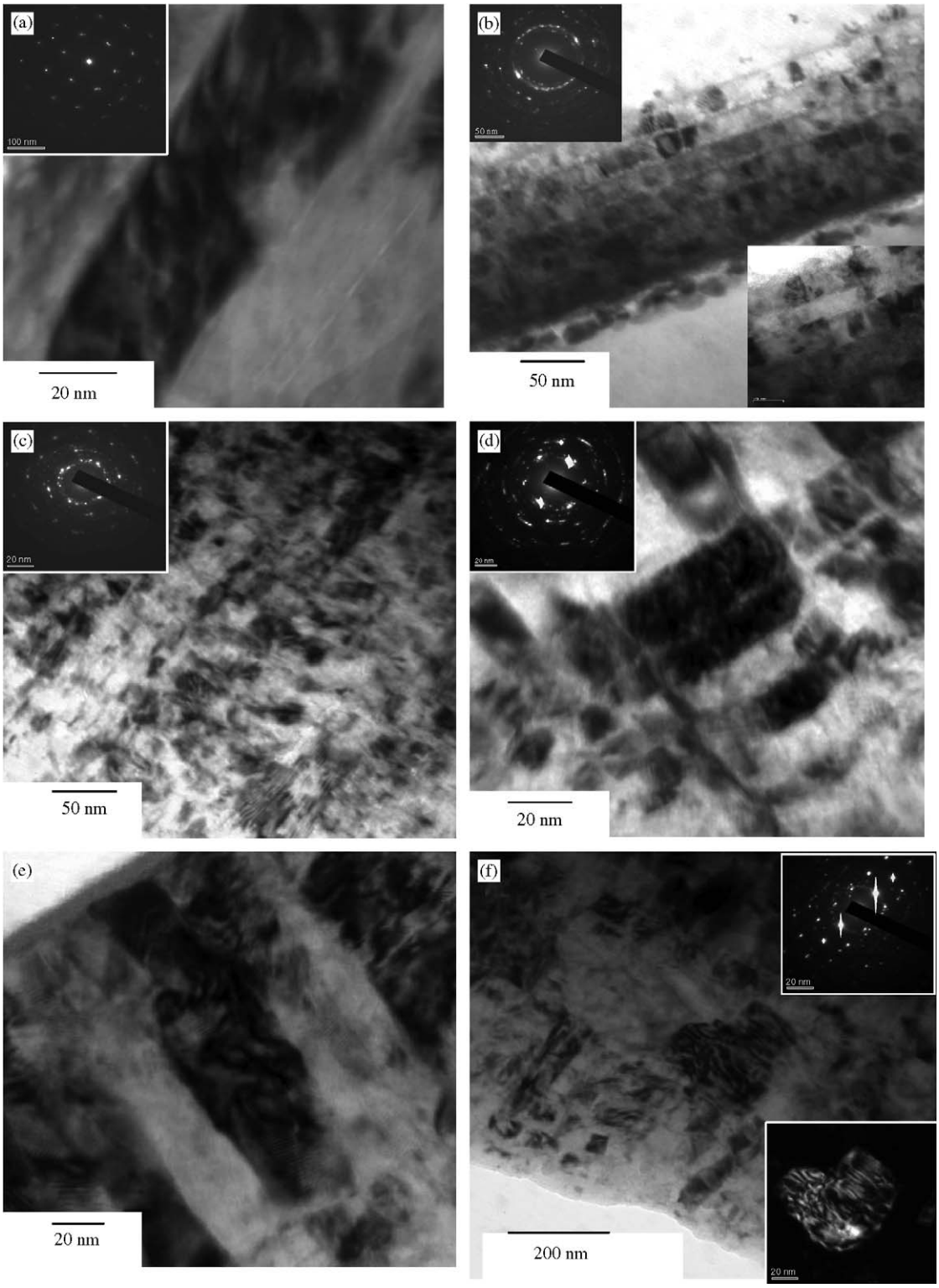

Fig. 4. Microstructures after 24 h at 773 K, (a) TiN, (b) TiN–CrN, (c) Ti–TiN, all in vacuum, and (d) Ti–TiN in air, and (e–f) Ti interlayer after annealing in vacuum and in air, respectively. All coatings were on Si substrate, with an interlayer spacing of 20 nm.

was no change in the trend in the failure mechanism with a change in the layer spacing, namely, in going from 100 to 20 nm. The TiN–CrN coating however showed a reverse trend with respect to substrate dependence as compared to that of monolayer TiN, namely, here the coating on the harder substrate, HCHCr, fails at a much higher load compared to that on Ti64, with L_c for HS718 falling in between (Fig. 8(b)) and hence this coating did not exhibit the invariance in L_c with respect to substrates as exhibited by Ti–TiN.

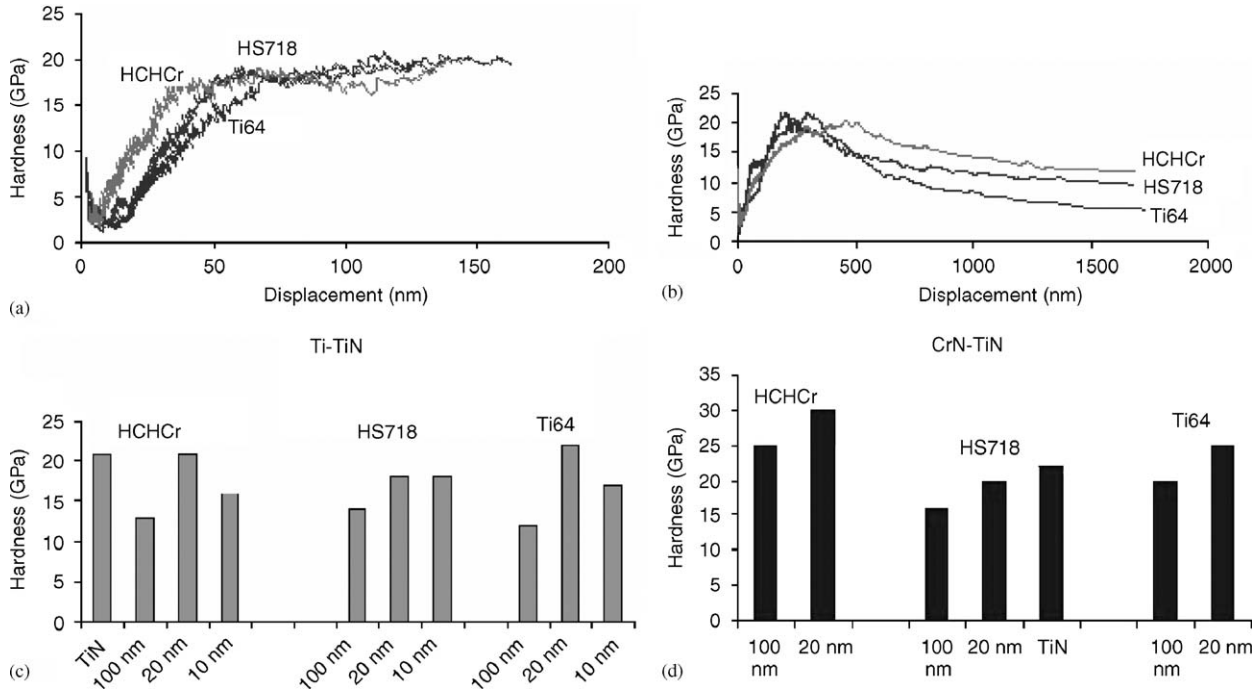

Fig. 5. Hardness of Ti–TiN (20 nm) on different substrates for indentation depths (a) less than 1/10th of the coating thickness, (b) higher than 1/10th of the coating thickness, comparative hardness plot of the coatings as a function of layer thickness on different substrates, for (c) Ti–TiN and (d) TiN–CrN.

Table 1
Hardness, critical load to failure and sliding wear rate, of the coatings on HCHCr substrate

Coating	Thickness (μm)	Layer thickness (nm)	Hardness (GPa)	Scratch adhesion critical load to failure (N)		Self-mated sliding wear wt. loss (mg)
				Onset	Total	
TiN	1.8	–	22	–	10.5	1.7
Ti–TiN	1.2	100	13	–	15	0.90
Ti–TiN	1.2	20	21	–	26	0.40
TiN–CrN	1.6	100	25	10	55	0.53
TiN–CrN	1.4	20	30	10	60	0.31

4.3. Tribological properties

The nanomultilayers outperformed the monolayer under dry sliding wear, both at room temperature and at 773 K. In both cases, a performance increment in wear has been observed with a decrease in interlayer spacing, as shown in Fig. 9(a), for the different coatings on a HCHCr substrate. The increase in wear resistance with a decrease in the interlayer spacing can be attributed to a direct application of Hall–Petch strengthening as well as the presence of several more interfaces, in the 20 nm interlayer coatings, as compared to the 100 nm ones. It is expected that these interfaces serve as regions with different dislocation mobilities and thereby lead to pile-ups that enable hardening of the material. It is however not very explicit as to what the interfaces do under a wear situation and has not been discussed in this study. The high temperature discs show a weight gain due to the formation of an incipient surface oxide layer. A comparative plot of the steady-state friction coefficients at room temperature is shown in Fig. 9(b). Increasing the temperature did not give rise to any appreciable difference in the friction coefficient values, and hence the plot of Fig. 9(b) shows the representative values at both room temperature and 773 K, in a single plot. The only difference between the two temperatures was in the initial friction coefficient values. The high-temperature wear tests showed all coatings, monolayer as well as multilayers, to start with an initially low-friction coefficient which later reached values comparable to what is representative of the two mating surfaces (steady state). Fig. 9(c) compares the variation of friction coefficient with sliding distance for all three coatings at 773 K to illustrate the above point. In contrast to the relationship between wear resistance and interlayer spacing, the friction coefficient remains nearly the same with change in interlayer spacing. This is because the two mating surfaces are experiencing the same volume of material even when there is a change in interlayer spacing. This is because the

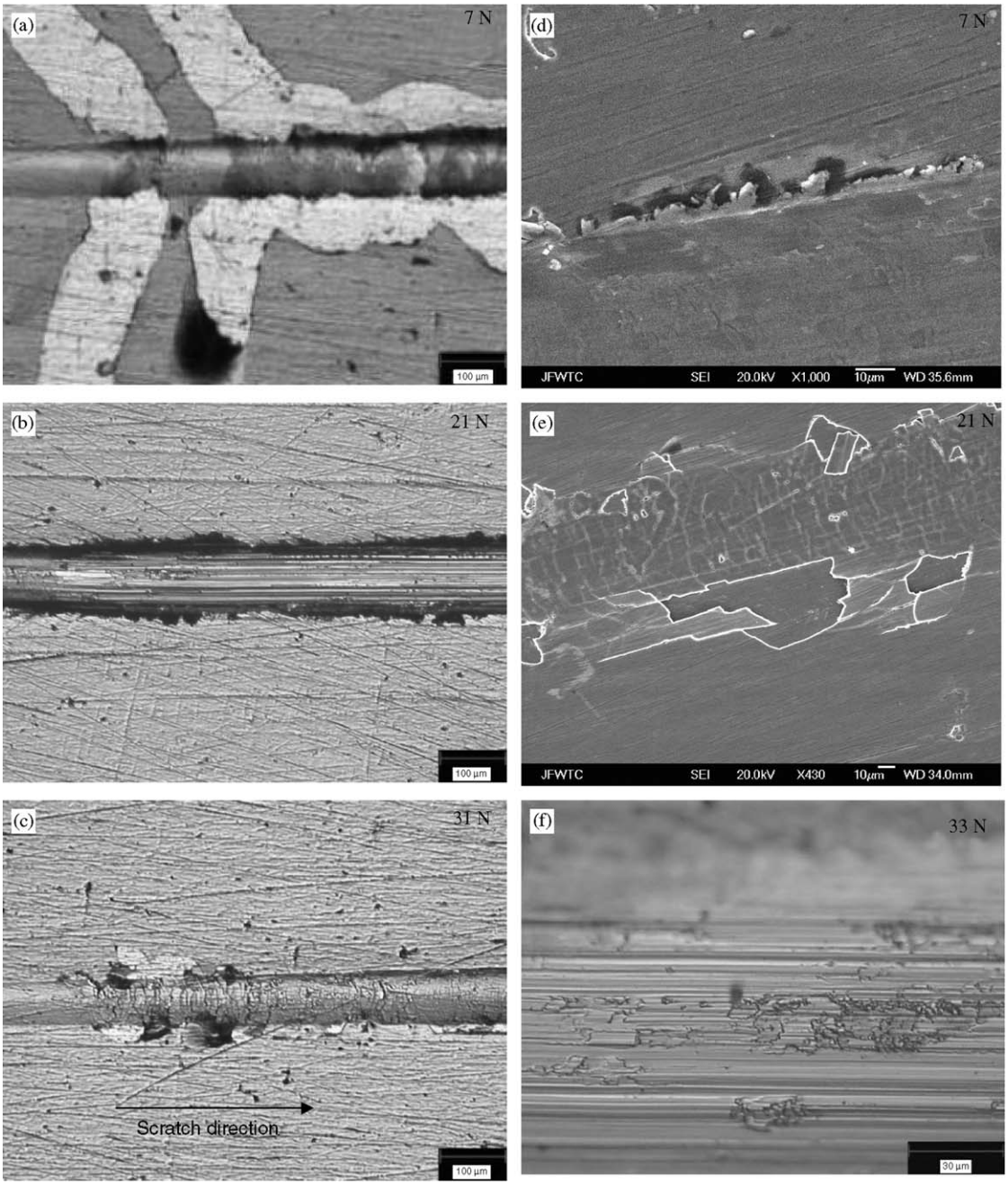

Fig. 6. Scratch tracks from (a) TiN, (b) Ti–TiN (20 nm) and (c) TiN–CrN (20 nm), on HS718, (d) failure in the monolayer showing initiation of edge flakes, followed by (e) peeling of the flake and (f) microcracks in the Ti–TiN multilayer track.

adhesive component of friction remains more or less unchanged as the mating surfaces are still nitride based, and the ploughing component of friction is not very significant for hard nitride coatings. However, there does exist a distinct signature when it comes to the time taken (namely, the distance covered) in reaching steady-state values. The initial low values in the high-temperature test are suspected to occur due to the formation of a thin oxide layer, and hence an uneven contact area between the disc and the pin. Once the multilayered coatings accumulate damage, they result in rupture of the uniform thin oxide layer. In addition, the high-flash temperatures at the contact area may lead to some softening of the mating surfaces, and hence yield a lubricating effect. However, as the test continues, the contact area increases making the surface less lubricious, representative of the actual friction between the two mating surfaces. An important point to note here is that the coatings do not undergo oxidation layer by layer, as wear takes place.

Amongst the three systems, the TiN–CrN multilayer coatings gave the least wear at both temperatures. The wear behaviour of the coatings on different substrates is

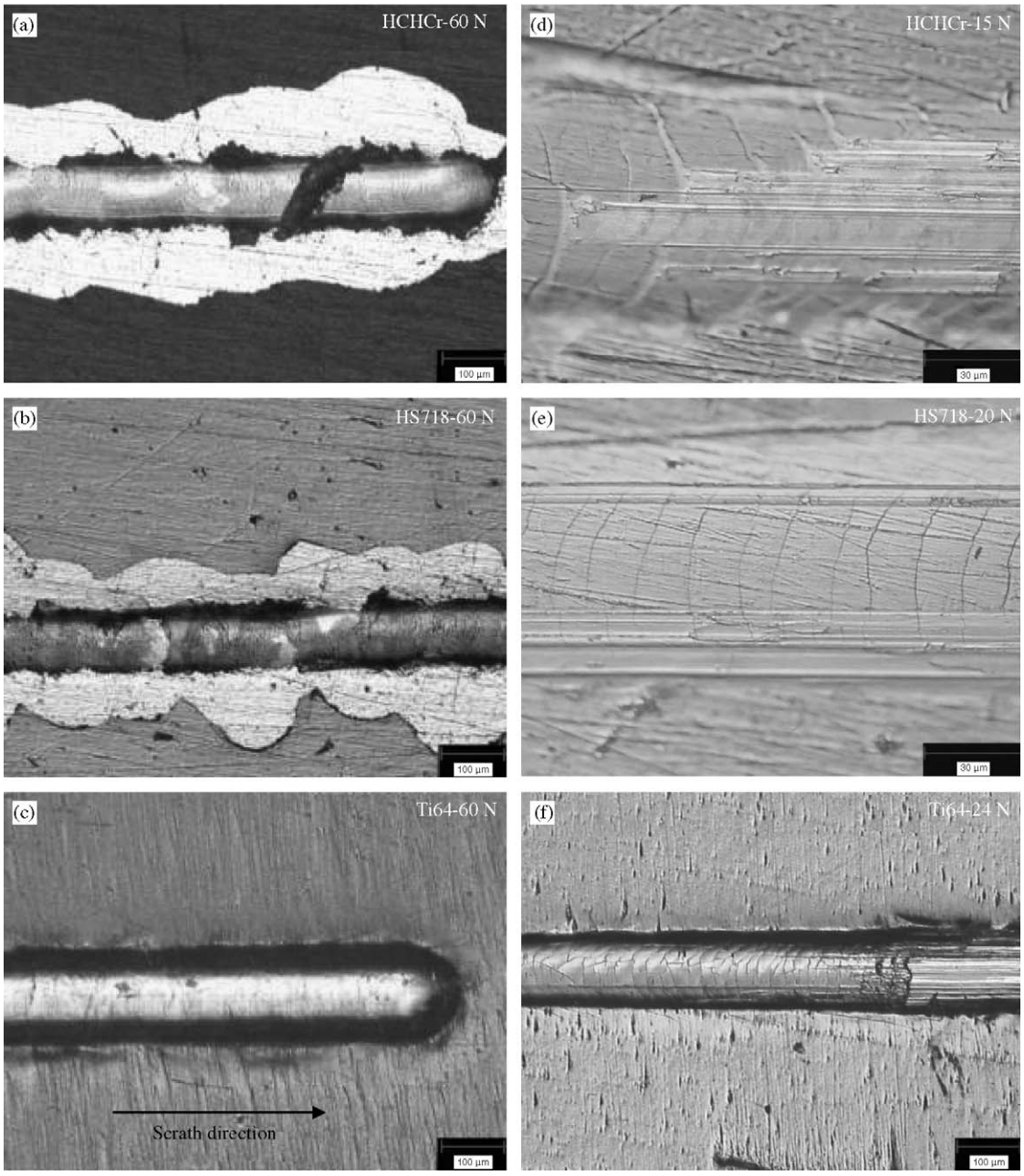

Fig. 7. Variation in the scratch failure mode with substrate type in (a–c) TiN and (d–f) Ti–TiN, on HCHCr, HS718 and Ti64 substrates, respectively.

however not so straight forward. By and large a maximum coating loss has been observed on the softer substrate, namely Ti64, for all three types of coatings (Fig. 9(d)) and between the two hard substrates it is somewhat difficult to spot any particular trend similar to that observed in the scratch test. The TiN monolayer experienced severe wear leading to catastrophic failure of the coating, as exhibited by the wear surface in Fig. 10(a), which shows the coating being ploughed through completely in most places. Here, there was no major change in the wear mechanism with a change in temperature (Fig. 10(b)). Examination of the worn pin (inset in Fig. 10(b)) shows the presence of TiN debris, especially filling the cavities in the pin. In the Ti–TiN multilayer, the room temperature test revealed that the coating has peeled off almost completely (Fig. 10(c)), however, the mechanism of wear was more uniform and gradual as compared to the monolayer, with distinct scoring marks (~8 μm wide) in the track. EDAX (inset) from the scored track reveals the presence of some remnant coating in many areas. At 773 K, the multilayer coating is nearly intact, with some evidence for incipient chipping along the edges (Fig. 10(d)). The smoothness of the Ti–TiN coating is contrasted to the flaking that takes place in the TiN–CrN coating, both at room temperature and at 773 K,

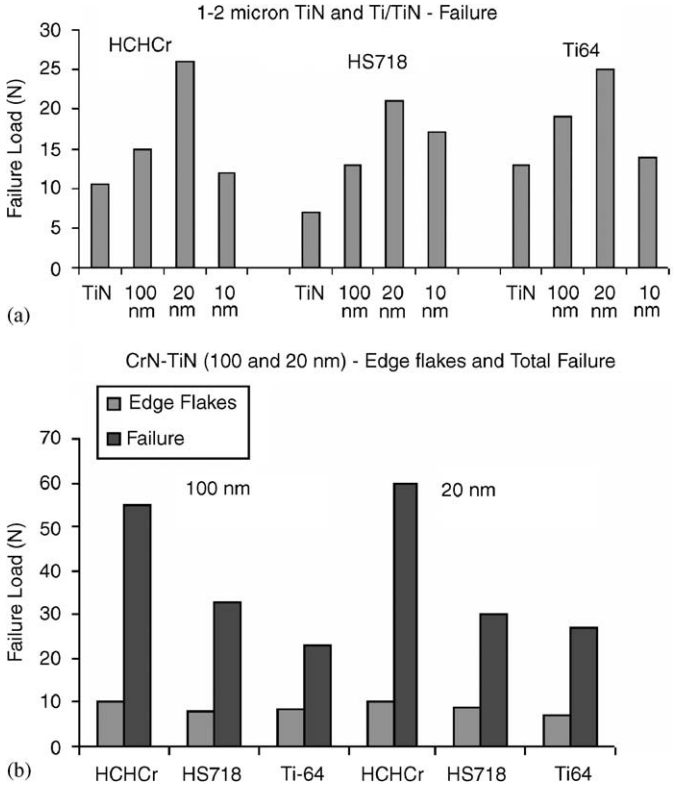

Fig. 8. Critical loads to coating failure as a function of layer thickness (20 and 100 nm) as well as substrate type (HCHCr, HS718 and Ti64); (a) TiN and Ti–TiN and (b) CrN–TiN.

as shown in Figs. 10(e) and (f), respectively. It is to be noted that despite no change in friction coefficient with change in the coating system and temperature, there is a noticeable change in the wear behaviour of the different coatings, which varies as a function of the test temperature.

5. Conclusions

This study demonstrates the thermal stability of nanomultilayer coatings at moderate temperatures. The coatings are thermally stable without any layer disintegration or oxidation or phase transformation, up to 24 h at 773 K. The nanomultilayers showed better properties as compared to the monolayer, both at room temperature and at 773 K. Decreasing the layer spacing from 100 to 20 nm always led to better hardness, scratch adhesion and wear resistance, at both temperatures. The coating hardness was independent of the substrate type, whereas under scratch testing the substrate plasticity was found to play an important role in determining the type of coating failure. Onset of failure occurred at a much higher load in the multilayers, indicative of a higher toughness. The harder substrates HS718 and HCHCr showed large amount of edge flakes whereas the softer substrate Ti64, showed practically no flaking and failed by the occurrence of total spallation ahead of the indentor in the case of monolayer TiN. The Ti–TiN multilayers, however, do not show any variation in the adhesion mechanism with respect

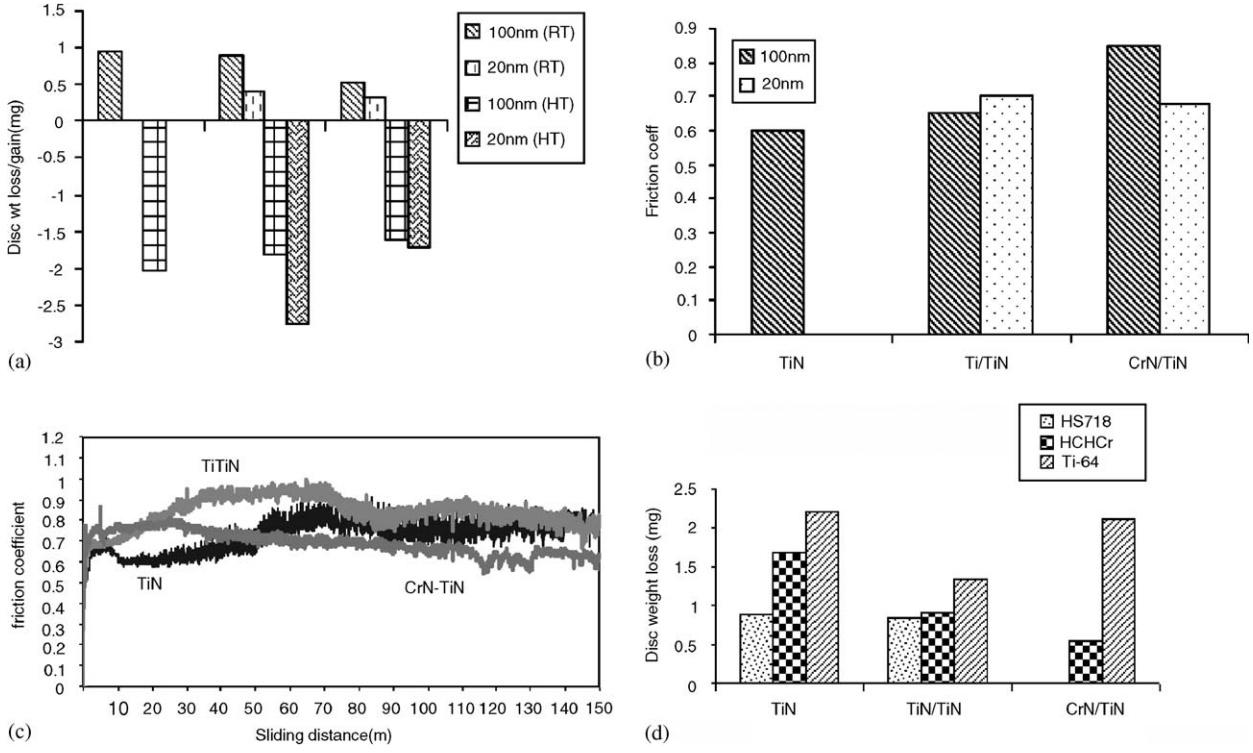

Fig. 9. Comparative plot showing (a) room temperature (weight loss) and high temperature (773 K) (weight gain) wear, (b) friction coefficient, of all three coatings at 773 K, (c) variation of friction coefficient with sliding distance at 773 K (20 nm) and (d) coating weight loss as a function of substrate type.

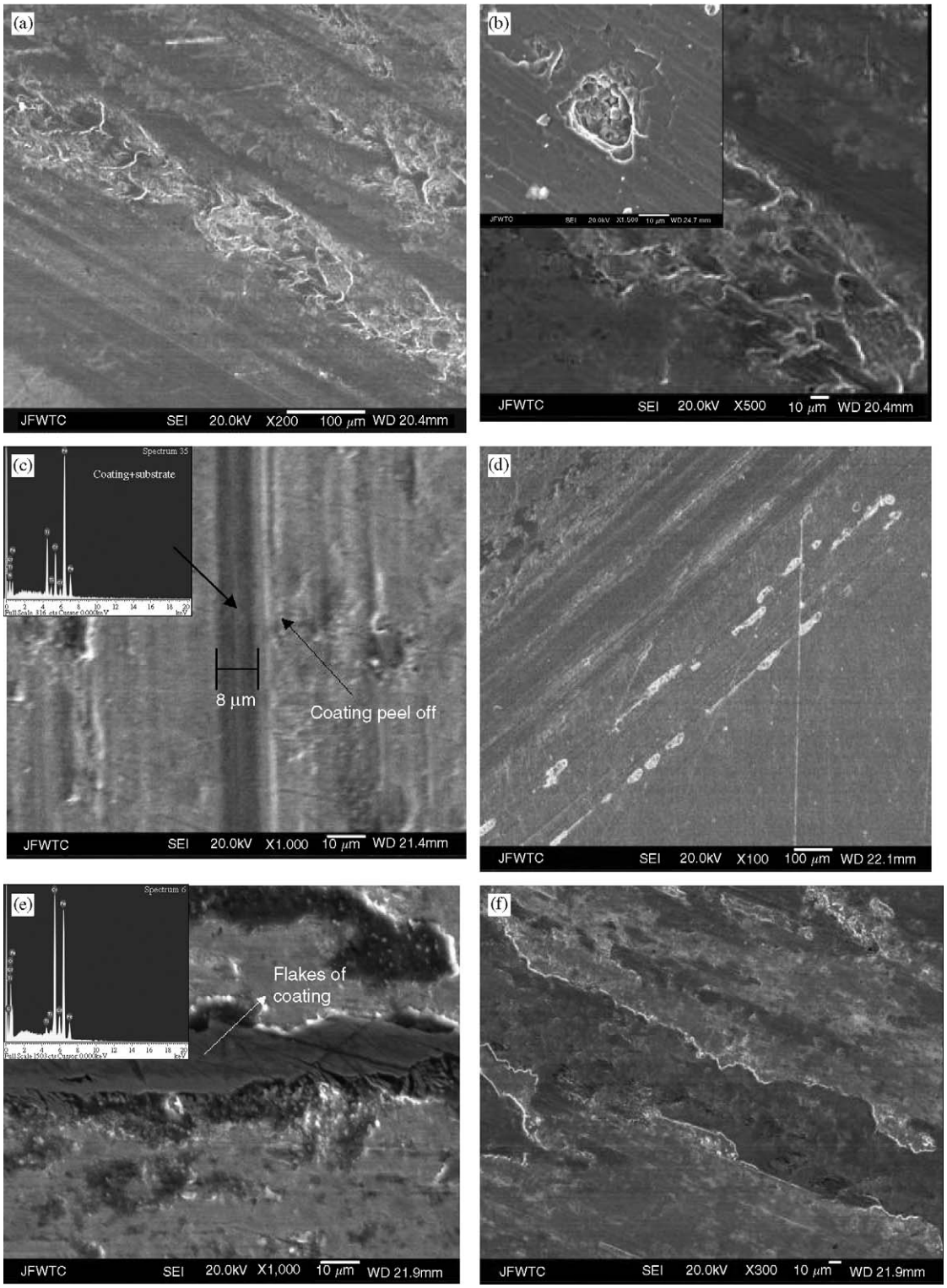

Fig. 10. Wear behaviour of TiN (a,b); Ti–TiN (c,d); and TiN–CrN (e,f) at room and high temperatures, respectively. Inset: cavities on the pin filled with wear debris, and EDAX showing the presence of the respective coating in the worn track.

to change in substrate type. The multilayers out-perform the monolayer under dry sliding wear, with the CrN–TiN system exhibiting a better response amongst the two. However, the mechanism of failure is more graceful in the Ti–TiN multilayers as compared to the CrN–TiN system indicative of a higher toughness. The nanomultilayer systems studied exhibit excellent thermal stability and tribological behaviour at 773 K.

Acknowledgements

This research was jointly supported by the global technology leader, ceramics and metallurgy technology, Christine Furstoss and the nanotechnology AT program of GE Global research, headed by Margaret Blohm.

References

[1] Ma KJ, Bloyce A, Bell T. Examination of mechanical properties and failure mechanisms of TiN and Ti–TiN multilayer coatings. Surf Coat Technol 1995;76–77:297–302.
[2] Wilson S, Alpas AT. Tribo-layer formation during sliding wear of TiN coatings. Wear 2000;245:223–9.
[3] Sundgren JE, Birch J, Hakansson G, Hultman L, Helmersson. Growth, structural characterization and properties of hard and wear protective layered materials. Thin Solid Films 1990;193/184:818–23.
[4] Holleck H, Schulz H. Advanced layer material constitution. Thin Solid Films 1990;153:11–8.
[5] Paldey S, Deevi SC. Single layer and multilayer wear resistant coatings of (Ti,Al)N: a review. Materials Science and Engineering 2003;A342:58–79.
[6] Wilkund U, Wanstrand O, Larsson M, Hogmark S. Evaluation of new multilayered physical vapour deposition coatings in sliding contact. Wear 1999;236:88–95.
[7] Chu X, Barnett SA, Wong MS, Sproul WD. Reactive unbalanced magnetron sputtered deposition of polycrystalline TiN/NbN superlattice coating. Surf Coat Technol 1993;57:13–8.
[8] Wilkund U, Hedenqvist P, Hogmark S. Mechanical and tribological characterization of DC magnetron sputtered tantalum nitride thin films. Surf Coat Technol 1997;97:773–85.
[9] Mori T, Fukuda S, Takemura Y. Improvement of mechanical properties of Ti/TiN multilayer film deposited by sputtering. Surf Coat Technol 2001;140:122–7.
[10] Bull SJ, Jones AM. Multilayer coatings for improved performance. Surf Coat Technol 1996;78:173–84.
[11] Kocker GM, Gross T, Santner E. Influence of the testing parameters on the tribological behaviour of self-mated PVD-coatings. Wear 1994;179:5–10.
[12] Habig KH. Friction and wear of sliding couples coated with TiC, TiN or TiB_2. Surf Coat Technol 1990;42:133–47.
[13] Nordin M, Larsosn M. Deposition and characterisation of multilayer PVD TiN/CrN coatings on cemented carbide. Surf Coatings Technol 1999;116–119:108–15.
[14] Zhou YM, Asaki R, Soe WH, Yamamoto R. Sliding wear behaviour of polycrystalline TiN.CrN multilayers against alumina ball. Surf Coatings Technol 2000;130:9–14.
[15] Sant C, Daia MB, Aubert P, Labdi S, Houdy P. Interface effect on tribological properties of titanium-titanium nitride nanolaminated structures. Surf Coat Technol 2000;127:167–73.

Further reading

[16] Larsson M, Bromark M, Hedenqvist P, Hogmark S. Deposition and mechanical properties of multilayered PVD Ti–TiN coatings. Surf Coat Technol 1995;76-77:202–5.